Accepted Manuscript

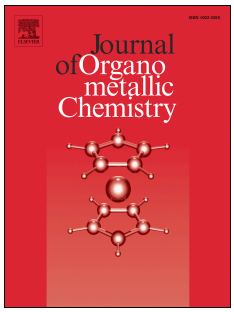

New salan and salen vanadium complexes: Syntheses and application in sulfoxidation catalysis

Minaxi S. Maru, Sónia Barroso, Pedro Adão, Luis G. Alves, Ana M. Martins

PII: S0022-328X(18)30481-9

DOI: 10.1016/j.jorganchem.2018.06.011

Reference: JOM 20470

To appear in: *Journal of Organometallic Chemistry*

Received Date: 20 April 2018

Revised Date: 1 June 2018

Accepted Date: 15 June 2018

Please cite this article as: M.S. Maru, Só. Barroso, P. Adão, L.G. Alves, A.M. Martins, New salan and salen vanadium complexes: Syntheses and application in sulfoxidation catalysis, *Journal of Organometallic Chemistry* (2018), doi: 10.1016/j.jorganchem.2018.06.011.

New Salan and Salen Vanadium Complexes: Syntheses and Application in Sulfoxidation Catalysis

Minaxi S. Maru, Sónia Barroso, Pedro Adão, Luis G. Alves and Ana M. Martins*

Centro de Química Estrutural, Instituto Superior Técnico, Universidade de Lisboa, Av. Rovisco Pais 1, 1049-001 Lisboa, Portugal

E-mail: ana.martins@tecnico.ulisboa.pt

Abstract

New diamine bis-phenol compounds of salan- (HOPh'CHNH$(CH_2)_2$NHCHPh'OH, Ph' = 2,4-$(CMe_2Ph)C_6H_2$, **H_2L1**) and salen-type (HOPh''CHN$(CHPh)_2$NCHPh''OH, Ph'' = 2,4-^{t}BuC_6H_2, **H_2L2** and HOPh''CHN(1,1'-2-binaphthyl)NCHPh''OH, Ph'' = 2,4-^{t}BuC_6H_2, **H_2L3**), as well as their oxido vanadium derivatives are described. VO(O^iPr)$_3$ was used as starting material for the preparation of [VO(O^iPr)(L1)], **1**, [VO(O^iPr)(L2)], **3**, and (μ-O){[VO(O^iPr)(μ-O)(L3)VO]}$_2$, **5**. An intramolecular redox process involving the reduction of V(V) to V(IV) converts **3** into [VO(L2)], **4**. The reactions of **1** and **5** with Me_3SiCl give [VOCl(L1)], **2**, and [VOCl(L3)], **6**, respectively. All complexes were tested as catalysts for the sulfoxidation of thioanisole using H_2O_2 as oxidant. In general, the compounds display high activity and selectivity, although salan-type complexes (**1** and **2**) perform better. Comparison of complexes **5** and **6** shows the monomeric species is more active and selective. Well-defined complexes, **5** and **6**, display better catalytic performance than systems using 1:1.5 [VO(acac)$_2$] and H_2L3.

Introduction

Sulfoxides are an important class of compounds that may be obtained by catalytic oxidation of thioethers using transition metal complexes as catalysts [1]. Among other early transition metals used, vanadium catalyzed sulfoxidation reactions gained prominence, as vanadium is a cheap metal, present in biological systems, and active when H_2O_2 is used as oxidant [2]. Despite the important contributions given to this research field, which include the implementation of bio-inorganic methodologies as well as successful kinetic resolution processes [3], the use of well-defined asymmetric sulfoxidation catalysts still presents several drawbacks [4]. The requirement of laborious and expensive separation procedures and the use of chlorinated solvents, low temperature and controlled addition of oxidants are some of the issues that need further development [4,5]. The implementation of new catalytic systems and a better understanding of their reactivity, through the identification of the species involved and the study of the reactions' mechanisms, using either computational or experimental methods, is thus an essential strategy to attain more efficient sulfoxidation systems.

As part of our research in transition metal catalyzed oxidation reactions [6], we focused on catalytic sulfoxidation of thioethers and described tripodal diamine bis(phenolate) oxidovanadium(V) complexes that are very selective (up to 98%) towards thioanisole sulfoxidation using H_2O_2 as oxidant, without requiring the use of chlorinated solvents [7,8].

Aiming to evaluate the properties of new vanadium complexes in sulfoxidation of thioanisole, we report here the synthesis of new salen- and salan-type vanadium complexes with different ligand frames as binaphthyl and phenyl groups, along with bulky o-phenolate substituents.

Results and Discussion

Synthesis and characterization

The ligand precursors used in this work are depicted in Figure 1. H_2L1 is a salan-type diamine bisphenol that was prepared by a single step Mannich condensation reaction of 2,4-$(CMe_2Ph)_2$PhOH, formaldehyde and ethylene diamine, adapting a literature procedure [9]. The ^{1}H and ^{13}C-{^{1}H} NMR spectra of H_2L1 are in agreement with a Cs-symmetric species, displaying only two sets of resonances for the Me and for the Ar-CH groups, one singlet for the ArCH_2N groups and one singlet for the NCH_2CH_2N moiety. H_2L2 and H_2L3 are salen-type diimine bisphenols that were synthesized through reactions of 3,5-di-tert-butyl-2-hydroxybenzaldehyde with the

corresponding diamines, following reported procedures [10]. H_2L3 was prepared from the racemic mixture of 1,1'-bi(2-naphthylamine), and H_2L2 was prepared from *meso*-(R,S)-diphenylethylenediamine.

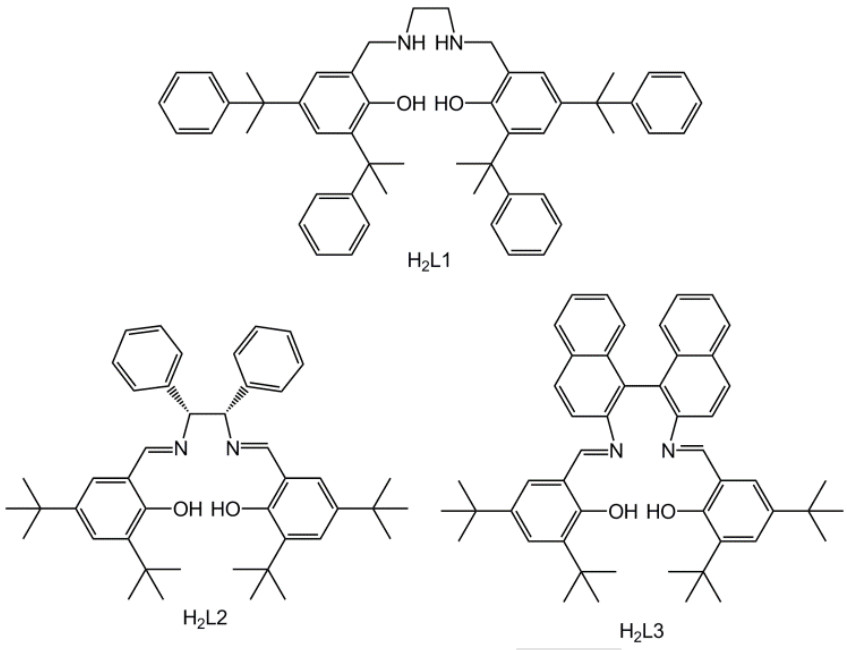

Figure 1. Ligand precursors used in this study

Crystals of H_2L2 suitable for X-ray diffraction were obtained by slow evaporation of an EtOH solution. The compound crystallizes in the monoclinic system, space group $P2_1/c$, with one half-molecule in the asymmetric unit. The structure is stabilized by the formation of intramolecular hydrogen bonds between the OH groups of the phenols and the N atoms of the diimine moieties. Such interactions display O(1)-H(1O)···N(1) bond lengths of 1.73(2) Å and define two 6-member heterocycles. The two phenyl rings linked to the two stereocenters of the molecule are placed in an anti periplanar conformation. The overall distances and angles fit the usual values reported in the literature for organic molecules [11].

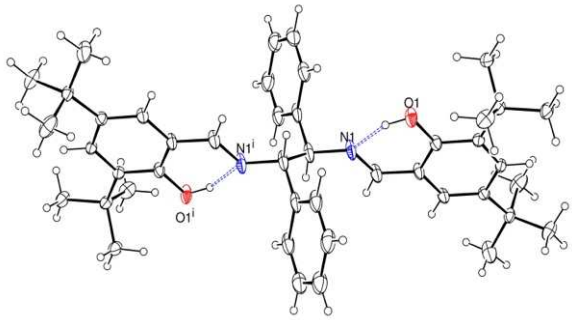

Figure 2. ORTEP diagram of H_2L2 using 30% probability level ellipsoids. Hydrogen bonds are represented by dashed lines. Equivalent atoms (^{i}) are generated using the symmetry transformation –x+1, -y, -z+2.

As shown in Scheme 1, treatment of $VO(O^iPr)_3$ with one equivalent of H_2L1 in THF at room temperature afforded [$VO(O^iPr)(L1)$], **1**, in 70% yield. The ^1H and ^{13}C-{^1H} NMR spectra of **1** revealed the formation of a *C1*-symmetric complex, displaying mutually-*trans* coordination of the phenolate rings to the metal. The ligand displays an overall *cis*-α coordination mode that is probably determined by the bulkiness of the dimethylphenyl substituents on the phenol groups [12]. As expected for an asymmetric species, the proton NMR spectrum of **1** displays 8 resonances for the Me groups of the CMe_2Ph moiety, 2 doublets and 1 septet for methyl and methyne protons of the isopropoxido ligand, 2 AX spin systems for the benzyl protons ArCH_2N, 4 doublets for the aromatic protons of

the phenol rings and several multiplets for the phenyl groups. The ^{51}V NMR spectrum of **1** in C_6D_6 displays one broad peak at δ -563 ppm, which is in agreement with the values reported for monomeric alkoxido oxidovanadium complexes supported by other amine phenolate donor sets [7,13].

The reaction of **1** with excess of Me_3SiCl in CH_2Cl_2 gave [VO(Cl)(L1)], **2**, in 60% yield (Scheme 1). The ^{1}H and ^{13}C-{^{1}H} NMR spectra of **2** are very similar to those of **1**, in agreement with a *C*1-symmetric species. The ^{51}V NMR spectrum of **2** displays one broad peak at δ -413 ppm in C_6D_6, which is in accordance with the values obtained for related complexes [7,12,13].

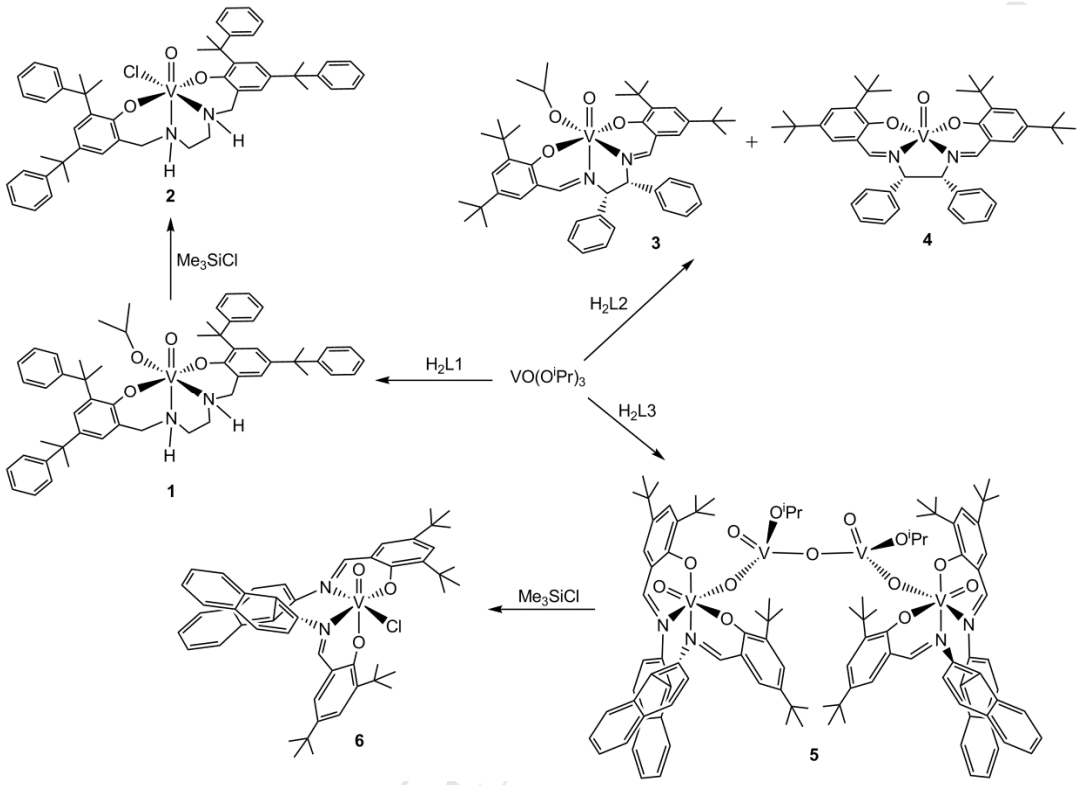

Scheme 1. Complexes synthesized

The reaction of VO(O^iPr)$_3$ with H_2L2 also led to the formation of a vanadium(V) complex, [VO(L2)(O^iPr)], **3**, but, together with this compound, a vanadium(IV) species, [VO(L2)], **4**, was also formed (Scheme 1). The reduction of V(V) to V(IV) is the result of a spontaneous intramolecular redox process that is accompanied by the oxidation of the isopropoxido ligand to acetone [14]. It is known that the V(V)O(salen)$^+$ species have a pronounced oxidative character, as evidenced by the highly positive V(V)O(salen)$^+$/V(IV)O(salen) and V(V)O(salen)$^+$/V(III)(salen)$^+$ redox couples [15]. Literature reports regarding the redox activity of isopropanol indicate that the onset of the oxidation to acetone can occur at potentials as low as 0.2 V vs. RHE (reversible hydrogen electrode) [16]. Therefore, the spontaneous oxidation of the isopropoxido ligand by the V(V)O(salen) core is possible from an electrochemical standpoint. Compound **3** and H_2L2 where identified by NMR but **4**, which is a d^1 species, was identified by single-crystal X-ray diffraction analysis of the crystals that grew in the bulk solution (see below). The ^{1}H and ^{13}C NMR spectra of **3** are consistent with its formulation as a C_1 symmetry species and the ^{51}V NMR resonance comes up at -479.9 ppm. The ESI-MS spectrum in CH_3CN shows a peak at m/z 709.70 (100%), that is assigned to [VO(L2)]$^+$.

Compound **4** was also independently synthesized in moderate yield by the reaction of $VOCl_2 \cdot 2H_2O$ with H_2L2. The first derivative of the EPR spectrum of **4**, measured in DMF at 77 K, is shown in Figure 3. The spin Hamiltonian parameters, g_{xy}= 1.977, g_z= 1.949, A_{xy}= 55.3 × 10^{-4} cm^{-1}, A_z= 160.6 × 10^{-4} cm^{-1}, were obtained by simulation of the experimental spectrum. The value obtained for the z-component of the hyperfine coupling constant, A_z, is consistent with the equatorial donor atom set of two imines and two phenolate oxygens [17].

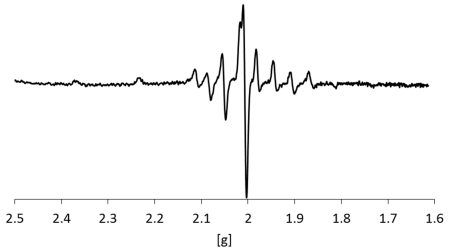

Figure 3. First derivative of the X-band EPR spectra of frozen solutions of **4**, measured at 77 K in DMF.

Compound **4** crystallizes in the triclinic system, *P*-1 space group, with two chemically identical but crystallographically independent molecules. An ORTEP diagram of one molecule is presented in Figure 4 and selected bond distances and angles are shown in Table 1. The coordination geometry of vanadium in **4** is square-pyramidal, typical of salen-type vanadium(IV) complexes. The basal plane is defined by the two nitrogen atoms and the two oxygen atoms of the salen ligand and the apical position is occupied with the oxido ligand. The bond distances V=O (1.597(5) Å), V-$O_{phenolate}$ (1.910(6) and 1.925(6) Å) and V-N_{imine} (2.036(7) and 2.052(8) Å) are within the ranges reported for other oxidovanadium(IV) complexes anchored by salen-type ligands [18].

Table 1. Selected bond lengths (Å) and angles (deg.) for compounds **4** and **5**.

	4	**5**
	Distances (Å)	
V(1)-N(1)	2.052(8)	2.325(7)
V(1)-N(2)	2.036(7)	2.147(7)
V(1)-O(1)	1.910(6)	1.846(5)
V(1)-O(2)	1.925(6)	1.896(6)
V(1)-O(3)	1.597(5)	1.601(5)
V(1)-O(4)	-	1.846(6)
V(2)-O(4)	-	1.725(6)
V(2)-O(5)	-	1.598(7)
V(2)-O(6)	-	1.766(2)
V(2)-O(7A)	-	1.715(7)
V1(1)-eq. pl[a]	0.598(3)	0.298(3)
	Angles (°)	
O(1)-V(1)-O(2)	89.4(3)	95.5(2)
O(1)-V(1)-O(3)	111.8(3)	103.2(2)
O(2)-V(1)-O(3)	107.0(3)	95.3(2)
O(4)-V(1)-O(1)	-	91.3(2)
O(4)-V(1)-O(2)	-	160.3(2)
O(3)-V(1)-O(4)	-	101.1(3)
O(1)-V(1)-N(1)	85.9(3)	82.8(2)
O(2)-V(1)-N(1)	148.5(2)	79.0(3)
O(3)-V(1)-N(1)	103.6(3)	172.2(3)
O(4)-V(1)-N(1)	-	83.6(3)
O(1)-V(1)-N(2)	139.8(3)	161.5(2)
O(2)-V(1)-N(2)	85.9(3)	82.1(3)
O(3)-V(1)-N(2)	107.6(3)	95.3(2)
O(4)-V(1)-N(2)	-	85.5(3)
N(1)-V(1)-N(2)	77.7(3)	78.7(2)
O(5)-V(2)-O(7A)	-	102.6(5)
O(5)-V(2)-O(4)	-	109.7(3)
O(7)-V(2)-O(4)	-	109.7(3)
O(5)-V(2)-O(6)	-	107.6(4)
O(7A)-V(2)-O(6)	-	109.9(4)
O(4)-V(2)-O(6)	-	112.1(3)
V(2)-O(6)-V(2[i])	-	177.6(6)
θ[b]	162.2(4)	120.0(3)

Equivalent atoms (^{i}) are generated using the symmetry transformation –x+1, y, -z+1/2.
[a] The equatorial plane is defined by atoms O1, O2, N1 and N2 in **4** and by O1, O2, O4 and N4 in **5**. [b] θ is the dihedral angle between the planes containing the phenolate rings.

The reaction of H_2L3 with VO(O^{i}Pr)$_3$ (Scheme 1) gives a mixture of several species. The analysis of 1D and 2D NMR data revealed the presence of free ligand and several minor vanadium species containing isopropoxido ligands. The major vanadium species is a rare tetranuclear vanadium(V) compound, (μ-O){[VO(O^{i}Pr)(μ-O)(L3)VO]}$_2$, **5**, which was identified by single-crystal X-ray diffraction (Figure 5) and by NMR. The ^{1}H and ^{13}C{^{1}H} NMR spectra of **5** are rather simple. In the (L3)V=O fragments the ligand is coordinated to the metal in the *cis*-β binding mode [12], and the NMR spectra show C_1 symmetry. The ^{1}H NMR spectrum displays 4 resonances for the *tert*-butyl substituents of the phenolate moieties, 2 singlets (δ 7.78 and 7.69 ppm) assigned to the N=CH protons, several singlets and multiplets in the aromatic region due to the phenolate and binaphthyl moieties and 1 septet and two doublets (δ 4.41, 0.88 and 0.39 ppm, respectively) due to the OCHMe$_2$ ligands. The ^{51}V NMR spectrum of **5** displays one small broad peak at δ -475 ppm assigned to [VO(L3)(O^{i}Pr)] and two intense peaks at δ -636 and -652 assigned to μ-oxido vanadium dimers. These assignments take into account the fact that replacing the chlorido ligand with more electronegative donors and increasing the steric bulk of the OR ligand coordinated to the V(V)O core shifts the ^{51}V signals upfield [19]. The values obtained are in agreement with those found for other oxidovanadium complexes supported by amine phenolate ligands [7,13].

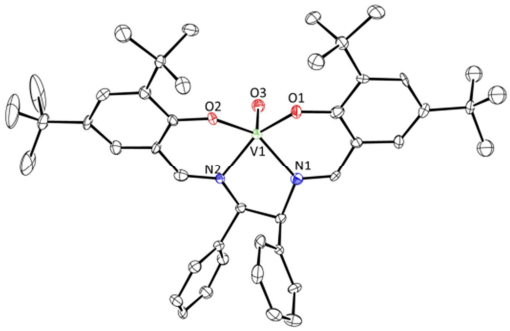

Figure 4. ORTEP diagram of **4** using 30% probability level ellipsoids. Hydrogen atoms are omitted for clarity.

Compound **5** crystallizes in the monoclinic system, *C*2/c space group, with half molecule of **5** and two co-crystallized molecules of Et_2O in the asymmetric unit. An ORTEP diagram of **5** is presented in Figure 5 and selected bond distances and angles are listed in Table 1. This is the first structurally characterized vanadium complex bearing a binaphthyl-based salen-type ligand. The coordination geometry around V1 is distorted octahedral with the equatorial plane defined by atoms O1, O2 and N2 of the salen ligand and the bridging oxygen atom O4, while the axial positions are occupied by the oxido ligand O3 and atom N3 of ligand L3. The coordination geometry of V2 is tetrahedral, defined by two bridging oxygen atoms, one terminal oxido ligand, and one oxygen atom of the isopropoxido ligand. Differently from other salen vanadium complexes, which display *trans*-phenolate moieties, the binding mode of L3 in **5** is *cis*-β.

The V=O (1.601(5) Å) and V-O$_{phenolate}$ (1.846(5) and 1.896(6) Å) bond distances are in agreement with the values reported for other oxidovanadium(V) complexes with salen ligands [20] while the V-N$_{imine}$ (2.325(7) and 2.147(7) Å) bond distances are longer than those reported in other oxidovanadium(V) complexes (typical values range from 2.054 to 2.114 Å) [21], possibly due to the *cis*-β binding mode of the ligand in **5**. The long V1-N1 bond distance, in comparison with V1-N2 (2.325(7) *vs*. 2.147(7) Å) is due to the *trans* effect of the oxido ligand O3. The V-O$_{bridging}$ bond lengths are in accordance with values reported [18, 20].

The appearance of a small signal in the ^{51}V NMR spectrum assigned to [VO(L3)(O^{i}Pr)] might be indicative that similarly to [VO(L2)(O^{i}Pr)], the compound is spontaneously reduced to V(IV). However, it is surprising that in the current experimental conditions, the final product is not the [VO(L3)] species, analogous to **4**, but a compound that may be described as a bridging oxido dimer of two divanadium moieties, namely (μ-O){[VO(O^{i}Pr)(μ-O)(L3)VO]}$_2$.

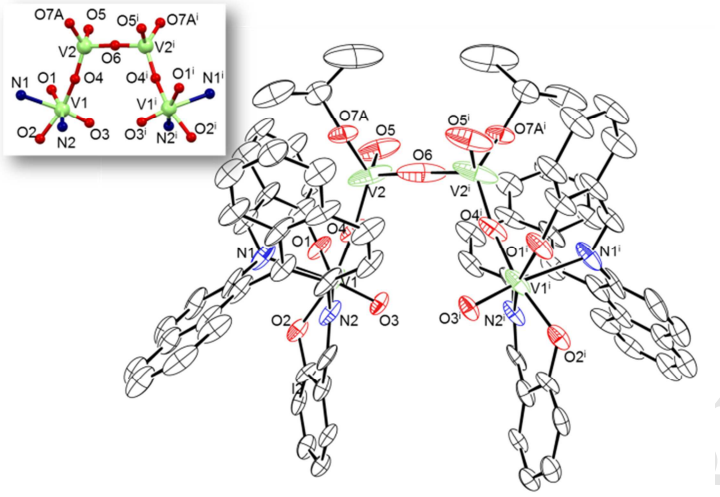

Figure 5. ORTEP diagram of **5** using 30% probability level ellipsoids. Hydrogen atoms, atoms belonging to B fraction of disordered isopropoxido ligand and *tert*-butyl substituents from phenolate groups are omitted for clarity. The inset shows the tetranuclear vanadium(V) core. Equivalent atoms (ⁱ) are generated using the symmetry transformation –x+1, y, -z+1/2.

The reaction of H_2L3 with $VO(O^iPr)_3$ in THF followed by addition of $SiMe_3Cl$ in CH_2Cl_2 led, upon recrystallization from n-hexane, to the isolation of pure [VO(L3)Cl], **6**, in 55% yield. The NMR spectra of **6** are in agreement with a C_1-symmetric species. The ^{1}H NMR spectrum displays 4 resonances for the CH_3 protons of the *tert*-butyl groups, 2 singlets at δ 8.07 and 8.06 ppm assigned to the N=CH protons and several multiplets in the range δ 7.81-8.06 ppm for the aromatic protons of the phenolate and binaphthyl moieties. The ^{51}V NMR spectrum of **6** displays one broad peak at δ -321 ppm in C_6D_6, which is in agreement with the values obtained for **1** and other chloride oxidovanadium(V) complexes supported by amine phenolate ligands [7,13].

Catalytic Studies

The vanadium complexes prepared were evaluated for their catalytic potential in the sulfoxidation of thioanisole. Control reactions were made to test for the lack of thioanisole oxidation in the absence of metal and confirm the role of vanadium complexes as catalysts. The results are listed in Table 2.

Using a ratio of 100:1 between substrate and catalyst precursor, all complexes led to high substrate conversions and product selectivity, although complexes [VO(X)(L1)], X = O^iPr, **1**, and X = Cl, **2**, present the best performances. Both compounds display the same catalytic features, which is not surprising considering that in the presence of H_2O_2 they should originate identical active species. The comparison of the solvents showed that in acetone the reactions are faster than in other solvents and, if the reaction is kept at 0 °C, the amounts of sulfone are, in general, very low. It is worth noting that complexes **1** and **2** afforded nearly complete conversions after 3 h at 0 °C. Comparatively, complex **6** exhibited a lower activity at 0 °C, with 85 % conversion after 3 h, although over oxidation to sulfone was not observed. Complexes **4** and **5** required longer reaction times in order to afford comparable conversions, although selectivities towards sulfoxide were lower. These results are in line with those previously reported for tripodal diamine bis(phenolate) vanadium complexes and, as observed for those systems, the reactions proceed without O_2 release [7].

The comparison between complexes **5** and **6** points out that the latter leads to a faster and more selective catalytic system. It is important to note that the inclusion of a binaphthyl moiety in the ancillary ligand frame of **6** led to 100% selectivity in sulfoxide. If, as expected, in the presence of H_2O_2 the V-O-V bridges of **5** are broken, the fragments resulting from the V1 centres may originate a catalytic active species that is close to the one formed from **6**, which implies that the lower selectivity obtained with **5** is likely associated to the V2 centres. Finally, it is clear that the *in situ* methodology (entries 11 and 12) affords comparable yields, but lower selectivities than the pre-formed complex **6**.

Table 2. Catalytic data for sulfoxidation of thioanisole[a]

Entry	Catalyst	Solvent	mol % cat.	T/ºC	*t* (h)	conv. (%)	sulfoxide (%)	sulfone (%)
1[b]	**1**	$(CH_3)_2CO$	1	0	3	99	93	6
2[c]	**1**	CH_3Cl_3	1	24	1	96	84	12
3[c]	**1**	EtOAc	1	24	1	93	73	20
4[c]	**1**	EtOH	1	24	1	97	82	15
5[b]	**2**	$(CH_3)_2CO$	1	0	3	>99	95	5
6[b]	**4**	$(CH_3)_2CO$	1	0	24	94	89	5
7[b]	**4**	DCE	1	0	24	88	84	4
8[b]	**5**	$(CH_3)_2CO$	1	0	24	93	78	15
9[b]	**5**	DCE	1	0	24	77	60	17
10[b]	**6**	$(CH_3)_2CO$	1	0	3	85	85	0
11[b]	**$VO(acac)_2/H_2L3$**	$(CH_3)_2CO$	1/1.5	0	24	97	87	10
12[b]	**$VO(acac)_2$/ H_2L3**	DCE	1/1.5	0	24	97	87	10

[a] Thioanisole (1 mmol); 1.2 eq. oxidant H_2O_2 20% (w/v) aqueous solution, 4 mL solvent.
[b] Conversion and yields determined by HPLC.
[c] Conversion and yields determined by NMR.

Concusions

[VO(X)(L1)], X = O^{i}Pr, **1**, and X = Cl, **2**, are salan-type diamine bisphenolate V(V) complexes that display very bulky dimethylphenyl substituents on the phenolate groups. Attempts to obtain pure [VO(O^{i}Pr)(L2)], **3**, and [VO(O^{i}Pr)(L3)], both displaying salen-type ligands, were hampered by spontaneous reduction to V(IV) via an intramolecular redox process that is accompanied by the oxidation of the isopropoxido ligand to acetone. Analysis of the literature reports concerning the redox activity of either V(V)O-(salen)X species and isopropanol indicates that this spontaneous intramolecular process is feasible [15,16]. In the case of L2, the resulting V(IV) complex is stable and displays a square-pyramidal geometry that is typical of vanadium(IV) oxido salen complexes. A more complex process leads to the formation of **5**. It may be speculated that transient formation of [VO(O^{i}Pr)(L3)] is followed by reduction to V(IV) by a process similar to the formation of **4**. However, this compound reacts further with $VO(O^iPr)_3$ to originate the tetra-vanadium complex (μ-O){[VO(O^{i}Pr)(μ-O)(L3)VO]}$_2$, **5**. [VO(Cl)(L3)], **6**, was obtained in more than 50% yield upon addition of Me_3SiCl to the mixture resulting from the reaction of H_2L3 and $VO(O^iPr)_3$.

In general, all complexes catalyse the sulfoxidation of thioanisole, although well-defined monomeric complexes, (**1**, **2** and **6**), display the better performances considering either activity and selectivity. It is noteworthy that the inclusion of the binaphthyl moiety in the ancillary ligand frame of **6** leads to 100% selectivity in sulfoxide.

The results also pointed out that the addition of salen-type ligand precursors to $VO(O^iPr)_3$, often used as vanadium(V) starting material for the syntheses of oxido vanadium complexes, led to concomitant reduction to V(IV). The latter may or not undergo subsequent reactions, leading to polynuclear vanadium complexes. These react with H_2O_2 to give V(V) species that are sulfoxidation catalysts. The higher selectivity displayed by monomeric precatalysts is likely associated to the presence of only one type of active species in solution.

Experimental Section

General

All reactions were carried out under inert atmosphere. Unless stated otherwise all reagents were purchased from commercial suppliers (e. g. Aldrich, Acrös, Fluka) and used as received. Chlorotrimethylsilane (TMSCl) was

distilled before use. THF, CH_2Cl_2 and n-hexane were dried by standard methods (sodium/benzophenone for THF; calcium hydride for CH_2Cl_2 and n-hexane) and distilled prior to use. H_2L3 was prepared following a literature procedure [10]. NMR samples of air/moisture sensitive compounds were prepared in a glovebox under inert atmosphere using NMR tubes equipped with J-Young stopcocks. C_6D_6 was dried over Na and distilled under reduced pressure. 1D NMR (^{1}H, ^{13}C-{^{1}H}, ^{13}C-{^{1}H} APT) and 2D NMR (COSY, NOESY, HSQC) spectra were recorded on Bruker Advance II+ 300 or 400 MHz (UltraShield Magnet) spectrometers, at ambient temperature. ^{1}H and ^{13}C chemical shifts (δ) are expressed in ppm relative to Me_4Si. EPR experiments were run in a Bruker EMX EPR Spectrometer and calibrated using a DPPH (2,2-diphenyl-1-picrylhydrazyl) solution as internal standard. The experimental spectra (1st derivative X-band EPR) were simulated with the computer program developed by Rockenbauer and Korecz [22]. The analysis of the products obtained in catalytic reactions was done by HPLC, using a Jasco system equipped with a Daicel Chiralpak IA column, a 870-UV Intelligent UV-Vis detector, two 880-PU Intelligent HPLC Pumps, a 2-line degasser 880-51 and a Rheodyne 725i injector (5 μL). The system uses Borwin software for data acquisition and analysis.

Synthesis of H_2L1

Ethylene diamine (0.901 g, 15 mmol) and 37 % aqueous solution formaldehyde (3.2 mL, 43.5 mmol) were added to a solution of 2,4-bis(2-phenylpropan-2-yl)phenol (10.9 g, 33 mmol) in EtOH (100 mL). The mixture was refluxed for 48h leading to an off-white solid precipitate that was filtered off, washed with cold ethanol and dried in vacuum. The solid was suspended in ethanol (50 mL) and the pH adjusted to <1 by dropwise addition of 6M HCl solution. The clear solution obtained was refluxed for 3 h and the solvent was then removed through evaporation. The residue was washed with Et_2O and dissolved in a 1:1 mixture of EtOH and water until a clear solution was obtained. The solution was then neutralized with a 1M Na_2CO_3 solution to give an off-white precipitate, which was filtered off, washed with ethanol and dried under vacuum (8.7 g, 78% yield). The product was recrystallized from CH_2Cl_2. ^{1}H NMR (400 MHz, C_6D_6, ppm): δ 7.32-7.28 (m, 8H, C*H*-Ar), 7.26 (d, $^4J_{HH}$ = 1.8 Hz, 2H, C*H*-Ar), 7.23-7.15 (m, 10H, C*H*-Ar), 7.12-7.07 (m, 2H, C*H*-Ar), 6.74 (d, $^4J_{HH}$ = 1.9 Hz, C*H*-Ar), 3.72 (s, 4H, ArCH_2N), 2.47 (s, 4H, N(CH_2)$_2$N), 1.72 (s, 12H, C(CH_3)$_2$Ph), 1.66 (s, 12H, C(CH_3)$_2$Ph). ^{13}C-{^{1}H} NMR (101 MHz, C_6D_6, ppm): δ 153.7, 151.43, 151.40, 140.3 and 135.5 (C_{ipso}-Ar), 128.0, 127.8, 126.9, 125.8, 125.7 and 125.6 (*C*H-Ar), 125.1 and 125.0 (*C*H-Ar), 121.8 (C_{ipso}-Ar), 52.6 (Ar*C*H$_2$N), 47.2 (N(*C*H$_2$)$_2$N), 42.6 and 42.1 (*C*(CH$_3$)$_2$Ph), 31.2 and 29.6 (C(*C*H$_3$)$_2$Ph). ESI-MS (CH_3CN): *m/z* = 745 (M^+), 100%. EA calcd. for $C_{52}H_{60}N_2O_2$·0.2(CH_2Cl_2): C, 82.28; H, 7.99; N, 3.68. Found: C, 82.34; H, 8.28; N, 3.65.

Synthesis of H_2L2

meso-1,2-diphenylethane-1,2-diamine (0.212 g, 1 mmol) was dissolved in 10 mL of EtOH and 3,5-di-tert-butyl-2-hydroxybenzaldehyde (0.469 g, 2 mmol) was then added. The mixture was refluxed for 20 h leading to a light yellow precipitate that was filtered off, washed with cold ethanol and dried under vacuum (0.412 g, 88%). Colourless crystals of H_2L2 suitable for X-ray diffraction were obtained by slow evaporation of an EtOH solution at room temperature. ^{1}H NMR (300 MHz, C_6D_6, ppm): δ 14.01 (s, 2H, O*H*), 7.83 (s, 2H, N=C*H*), 7.56 (d, 2H, $^4J_{HH}$ = 1.9 Hz, C*H*-Ar), 7.28 (m, 4H, C*H*-Ph), 7.07 (m, 4H, C*H*-Ph), 6.98 (m, 2H, C*H*-Ph), 6.88 (d, 2H, $^4J_{HH}$ = 2.1 Hz, C*H*-Ar), 4.54 (s, 2H, NC*H*), 1.64 (s, 18H, C(CH_3)$_3$), 1.28 (s, 18H, C(CH_3)$_3$). ^{13}C-{^{1}H} NMR (101 MHz, C_6D_6, ppm): δ 167.3 (N=CH), 158.8, 140.3, 140.1, 137.1 (C_{ipso}-Ar), 128.6, 127.9, 127.5, 126.9 (*C*H-Ar), 118.6 (C_{ipso}-Ar), 80.2 (N-*C*H), 35.5 and 34.3 (*C*(CH$_3$)$_3$), 31.7 and 29.8 (C(*C*H$_3$)$_3$). EA calcd. for $C_{44}H_{56}N_2O_2$: C, 81.94; H, 8.75; N, 4.34. Found: C, 81.75; H, 9.09; N, 4.35. ESI-MS (CH_3CN): *m/z* = 416 (M^+), 100%.

*Synthesis of [VO(L1)(O^{i}Pr)], **1***

A THF solution of VO(O^{i}Pr)$_3$ (0.244 g, 1 mmol) was added dropwise, with continuous stirring at room temperature, to a solution of H_2L1 (0.744 g, 1 mmol) in the same solvent. The initially colorless solution turned dark purple while it was stirred for 18 h, after which the solvent was evaporated to dryness. The compound was recrystallized from n-hexane at –20 °C to give a purple crystalline solid (0.608 g, 70 % yield). ^{1}H NMR (300 MHz, C_6D_6, ppm): δ 7.56 (d, $^4J_{HH}$ = 1.9 Hz, 1H, C*H*-Ar), 7.51 (d, $^4J_{HH}$ = 2.1 Hz, 1H, C*H*-Ar), 7.46-7.41 (m, 2H, C*H*-Ar), 7.39-7.28 (m, 4H, C*H*-Ar), 7.26-7.18 (m, 6H, C*H*-Ar), 7.11-7.02 (m, 2H, C*H*-Ar), 6.95 (d, $^4J_{HH}$ = 2.4 Hz, 1H, C*H*-Ar), 6.96-6.86 (m, 4H, C*H*-Ar), 6.84 (d, $^4J_{HH}$ = 1.9 Hz, 1H, C*H*-Ar), 6.81-6.72 (m, 2H), 5.88 (sept, $^3J_{HH}$ = 6.1 Hz, 1H, C*H*(CH$_3$)$_2$), 4.66 (d, $^2J_{HH}$ = 12.5 Hz, 1H, NCH_2Ar), 4.33 (d, $^2J_{HH}$ = 13.7 Hz, 1H, NCH_2Ar), 3.16 (d, $^2J_{HH}$ = 14.1 Hz, 1H, NCH_2Ar), 2.89 (d, $^2J_{HH}$ = 14.3 Hz, 1H, NCH_2Ar), 2.18 (s, 3H, C(CH_3)$_2$Ph), 1.90 (s, 3H, C(CH_3)$_2$Ph), 1.81 (s, 3H, C(CH_3)$_2$Ph), 1.79 (s, 3H, C(CH_3)$_2$Ph), 1.74 (s, 3H, C(CH_3)$_2$Ph), 1.73 (s, 3H, C(CH_3)$_2$Ph), 1.52 (s, 6H, C(CH_3)$_2$Ph), 1.48 (m, 2H, N(CH_2)$_2$N), 1.43 (d, $^3J_{HH}$ = 6.1 Hz, 3H, CH(CH_3)$_2$), 1.37 (m, 2H, N(CH_2)$_2$N), 1.34 (d, $^3J_{HH}$ = 6.1 Hz, 3H, CH(CH_3)$_2$). ^{13}C-{^{1}H} NMR (101 MHz, C_6D_6, ppm): δ 154.8, 154.3, 151.9, 151.6, 140.0 and 139.6 (C_{ipso}-Ar), 128.5, 127.4, 127.3, 127.2, 126.7, 126.5, 126.2, 126.0, 125.9, 124.1, 124.0, 123.5 and 123.3 (*C*H-Ar), 122.9 (C_{ipso}-Ar), 85.2 (*C*H(CH$_3$)$_2$), 56.1 and 52.3 (NCH$_2$Ar), 45.8 and 43.6 (N(CH_2)$_2$N), 42.92, 42.88,

42.7 and 42.5 ($C(CH_3)_2Ph$), 33.0, 32.7, 31.6, 31.6, 31.5, 31.5, 26.1 and 26.0 ($C(CH_3)_2Ph$), 25.9 and 25.8 ($CH(CH_3)_2$). ^{51}V NMR (79 MHz, C_6D_6, ppm): δ -563.4. FT-IR (KBr, cm^{-1}): ν(V=O) 801. EA calcd. for $C_{55}H_{65}N_2O_4V{\cdot}0.6(CH_2Cl_2)$: C, 72.59; H, 7.25; N, 3.04. Found: C, 72.54; H, 7.44; N, 3.10. ESI-MS (CH_3CN): *m/z* = 809.53 $[V^{V}O(L1)]^+$, *ca*. 70%; 849.86 (M^+), 100%; 1636.13 $\{[V^{V}O(L1)]_2O\}^+$, *ca*. 20%.

Synthesis of [VO(L1)Cl], ***2***

1 (0.608 g, 0.7 mmol) was suspended in 10 mL of CH_2Cl_2 and three equivalents of $SiMe_3Cl$ (0.179 g, 2.1 mmol) were added dropwise at room temperature. The mixture was stirred for 18 h to give a dark violet solution. The solvent was evaporated to dryness under vacuum to give a dark violet powder that was recrystallized from n-hexane at -20 °C (0.355 g, 60 % yield. ^1H NMR (300 MHz, C_6D_6, ppm): δ 7.61 (s, 1H, C*H*-Ar), 7.46-7.31 (m, 7H, C*H*-Ar), 7.25-7.17 (m, 6H, C*H*-Ar), 7.10-7.04 (m, 2H, C*H*-Ar), 6.97-6.89 (m, 2H, C*H*-Ar), 6.87-6.64 (m, 5H, C*H*-Ar), 6.58-6.53 (m, 1H, C*H*-Ar), 4.92 (d, $^2J_{HH}$ = 14.1 Hz, 1H, NCH_2Ar), 4.52 (d, $^2J_{HH}$ = 13.7 Hz, 1H, NCH_2Ar), 3.08 (d, $^2J_{HH}$ = 14.5 Hz, 1H, NCH_2Ar), 2.84 (d, $^2J_{HH}$ = 14.5 Hz, 1H, NCH_2Ar), 2.10 (s, 3H, $C(CH_3)_2Ph$), 2.05 (s, 3H, $C(CH_3)_2Ph$), 1.79 (s, 3H, $C(CH_3)_2Ph$), 1.77 (s, 3H, $C(CH_3)_2Ph$), 1.70 (s, 3H, $C(CH_3)_2Ph$), 1.68 (s, 3H, $C(CH_3)_2Ph$), 1.49 (s, 3H, $C(CH_3)_2Ph$), 1.36 (m, 1H, $N(CH_2)_2N$), 1.36 (s, 3H, $C(CH_3)_2Ph$), 1.32 (m, 2H, $N(CH_2)_2N$), 1.18 (m, 1H, $N(CH_2)_2N$). ^{13}C-{^1H} NMR (101 MHz, C_6D_6, ppm): δ 162.1, 159.0, 154.4, 153.8, 150.9, 146.0, 141.8, 137.5 and 136.3 (C_{ipso}-Ar), 128.6, 128.5, 127.2, 127.1, 126.7, 126.5, 126.3, 126.2, 126.1, 124.4, 124.1, 123.8 and 123.3 (*C*H-Ar), 119.2 (C_{ipso}-Ar), 57.8 and 52.0 (NCH_2Ar), 47.1 and 44.3 ($N(CH_2)_2N$), 43.2, 43.0, 42.8 and 42.6 ($C(CH_3)_2Ph$), 32.7, 32.6, 31.6, 31.3, 26.6 and 26.1 ($C(CH_3)_2Ph$). ^{51}V NMR (79 MHz, C_6D_6, ppm): δ -413. FT-IR (KBr, cm^{-1}): ν(V=O) 802. EA calcd. for $C_{52}H_{58}ClN_2O_3V{\cdot}2.8(CH_2Cl_2)$: C, 60.76; H, 5.92; N, 2.59. Found: C, 60.61; H, 6.33; N, 2.56. ESI-MS (CH_3CN): *m/z* = 843.01 (M^-), 100%; 878.58 $\{[V^{V}O(L1)(Cl)]Cl\}^-$, *ca*. 45%; 905.65 $\{[V^{V}O_2(H_2L1)Cl]CH_3CN\}^-$, *ca*. 40%.

Reaction of H_2L2 with $VO(O^iPr)_3$

A THF solution of $VO(O^iPr)_3$ (0.122 g, 0.5 mmol) was added dropwise to a solution of H_2L2 (0.318 g, 0.5 mmol) in the same solvent, at room temperature. The initially colorless solution turned to dark blue and, after being stirred for 18 h, it was evaporated to dryness to give a blue crystalline powder. A THF solution of the powder at -20 ºC gave green crystals of **4** suitable for X-ray diffraction. The NMR analysis of the remaining solid revealed the presence of H_2L2 and [VO(L2)(O^iPr)], **3**, in 1:4 ratio. Data for **3**: ^1H NMR (300 MHz, $CDCl_3$, ppm): δ 8.29 (s, 1H, N=C*H*), 8.14 (s, 1H, N=C*H*), 7.56 (s, 2H, C*H*-Ar), 7.40-7.14 (m, 4H, C*H*-Ph), 7.07 (2H, C*H*-Ar), 7.04-6.93 (m, 4H C*H*-Ph), 6.57 (m, 2H, C*H*-Ph), 6.35 (d, J = 6.0 Hz, 1H, NC*H*), 6.20 (sept, $^3J_{HH}$ = 6.0 Hz, 1H, OC*H*$(CH_3)_2$), 5.03 (d, $^3J_{HH}$ = 6.0 Hz, 1H, NC*H*), 1.61 (s, 9H, $C(CH_3)_3$), 1.48 (s, 9H, $C(CH_3)_3$), 1.44 (d, 3H, $CH(CH_3)_2$), 1.30 (s, 9H, $C(CH_3)_3$), 1.26 (s, 9H, $C(CH_3)_3$), 1.24 (d, 3H, $CH(CH_3)_2$). ^{13}C-{^1H} NMR (101 MHz, C_6D_6, ppm): δ 167.0 (N=*C*H), 166.8 (C_{ipso}-Ar), 160.7 (N=*C*H), 158.1, 141.3, 139.4, 138.9, 138.4 and 132.3 (C_{ipso}-Ar), 132.1 (CH-Ph), 130.44 (CH-Ar), 129.6 (CH-Ph), 129.2, 129.0 and 128.9 (CH-Ar), 128.54, 128.45, 128.4, 128.3, 128.2 and 125.7 (CH-Ph), 122.3 and 121.8 (C_{ipso}-Ph), 89.6 ($CH(CH_3)_2$), 76.1 and 75.4 (NCH), 35.69, 35.68, 34.4 and 34.3 ($C(CH_3)_3$), 31.6, 31.5, 30.5 and 30.2 ($C(CH_3)_3$), 26.6 and 26.4 ($CH(CH_3)_2$). ^{51}V NMR (79 MHz, C_6D_6, ppm): δ –480. ESI-MS (CH_3CN): *m/z* = 709.70 $[V^{V}O(L1)]^+$, 100%.

Synthesis of [VO(L2)], ***4***

H_2L2 (0.432 g, 0.67 mmol) in EtOH was added to an aqueous solution 50 % (w/v) of $VOCl_2{\cdot}2H_2O$ (0.18 mL, 0.67 mmol) and the mixture was stirred for 0.5 h at room temperature leading to a green/grey solution. Addition of a solution of NaOH 1M in water till pH ~ 8 led to the formation of a light green precipitate that was separated by filtration and dried in vacuum (0.290 g, 61%). EPR (DMF, 77 K): g_z= 1.949, A_z= 160.6 × 10^{-4} cm^{-1}. Elemental analysis: Calcd. for $C_{44}H_{54}N_2O_3V{\cdot}0.8(H_2O)$; C, 72.97; H, 7.74; N, 3.87; Found: C, 72.96; H, 7.24; N, 3.82.

Reaction of H_2L3 with $VO(O^iPr)_3$

A THF solution of $VO(O^iPr)_3$ (0.122 g, 0.5 mmol) was added dropwise to a solution of H_2L3 (0.406 g, 0.5 mmol) in the same solvent, at room temperature. The initially colorless solution turned to dark blue and, after 18 h, it was evaporated to dryness to give a blue crystalline powder. The NMR analysis of the powder revealed the presence of several species including H_2L3, [VO(L3)(O^iPr)] and (μ-O){[VO(O^iPr)(μ-O)(L3)VO]}$_2$,**5**. An Et_2O solution of the mixture at -20 ºC gave blue crystals of **5** in 30% yield, suitable for X-ray diffraction. Data for **5**: ^1H NMR (300 MHz, C_6D_6, ppm): δ 9.25 (d, J = 8.5 Hz, 1H, C*H*-Ar), 8.48 (d, J = 8.4 Hz, 1H, C*H*-Ar), 8.34 (d, J = 8.5 Hz, 1H, C*H*-Ar), 7.88 (s, 1H, N=C*H*), 7.76 (s, 1H, C*H*-Ar), 7.69 (s, 1H, N=C*H*), 7.58 (s, 2H, C*H*-Ar), 7.36-7.18 (m, 4H, C*H*-Ar), 7.04-6.86 (m, 3H C*H*-Ar), 6.81 (d, J = 8.5 Hz, 2H, C*H*-Ar), 6.62 (s, 1H, C*H*-Ar), 4.41 (sept, $^3J_{HH}$ = 6.1 Hz, 2H, OC*H*$(CH_3)_2$), 2.19 (s, 18H, $C(CH_3)_3$), 1.72 (s, 9H, $C(CH_3)_3$), 1.29 (s, 9H, $C(CH_3)_3$), 1.04 (s, 9H, $C(CH_3)_3$), 0.88 (d, 6H, $CH(CH_3)_2$), 0.39 (d, 6H, $CH(CH_3)_2$). ^{13}C-{^1H} NMR (101 MHz, C_6D_6, ppm): δ 168.0 and 166.2 (C_{ipso}-Ar), 165.7

and 164.1 (N=*C*H), 149.6, 149.2, 144.4, 141.1, 137.8, 136.1 134.0, 133.6, 133.4 (C_{ipso}-Ar), 132.2 (CH-Ar), 132.1 (C_{ipso}-Ar), 130.9, 129.8, 129.4, 128.6, 127.1, 127.0, 126.7, 126.4 and 125.4 (CH-Ar), 125.2 and 125.1 (C_{ipso}-Ar), 124.7 (CH-Ar), 119.9 (C_{ipso}-Ar), 82.6 ($CH(CH_3)_2$), 36.3, 35.8, 34.7 and 34.2 ($C(CH_3)_3$), 31.6, 31.4, 30.8 and 30.4 ($C(CH_3)_3$), 25.9 and 25.3 ($CH(CH_3)_2$). ^{51}V NMR (79 MHz, C_6D_6, ppm): δ –475, –636, –652. ESI-MS (CH_3CN): *m/z* = 781.55 $[V^VO(L2)]^+$, 100%.

Synthesis of [VO(L3)Cl], ***6***

A solution of H_2L3 (0.500 g, 0.7 mmol) in THF was slowly added to a solution of $VO(O^iPr)_3$ (0.171 g, 0.7 mmol) in the same solvent and stirred for 18 h at room temperature. The solvent was removed under reduced pressure and the dark blue powder that formed was suspended in 10 mL of CH_2Cl_2. $SiMe_3Cl$ (0.179 g, 2.1 mmol) was then added dropwise to the suspension and the mixture was stirred at room temperature for 18 h. The solvent was evaporated under reduced pressure and the dark blue residue dried under vacuum. The compound was recrystallized from n-hexane at -20 ºC (0.321 g, 55 % yield). ^{1}H NMR (300 MHz, C_6D_6, ppm): δ 8.07 (s, 1H, N=C*H*), 8.06 (s, 1H, N=C*H*), 7.81-7.55 (m, 6H, C*H*-Ar), 7.44-7.22 (d, 3H, C*H*-Ar), 7.13 (m, 1H, C*H*-Ar), 6.99 (m, 1H, C*H*-Ar), 6.93-6.76 (m, 5H, C*H*-Ar), 1.81 (s, 9H, $C(CH_3)_3$), 1.58 (s, 9H, $C(CH_3)_3$), 1.16 (s, 9H, $C(CH_3)_3$), 1.00 (s, 9H, $C(CH_3)_3$). ^{13}C-{^{1}H} NMR (101 MHz, C_6D_6, ppm): *δ* 168.4 and 167.0 (C_{ipso}-Ar), 165.53 and 165.49 (N=*C*H), 150.2, 149.3, 145.7, 142.2, 136.6, 134.7, 132.9, 132.8, 132.5 and 131.9 (C_{ipso}-Ar), 130.9, 129.3, 128.7, 128.5, 128.4, 128.2 and 126.9 (*C*H-Ar), 126.9 (C_{ipso}-Ar), 126.7, 126.6, 126.53 and 126.49 (*C*H-Ar), 125.9 (C_{ipso}-Ar), 125.6, 125.2, 125.1 and 124.7 (*C*H-Ar), 124.1 and 120.2 (C_{ipso}-Ar), 35.5, 35.1, 34.3 and 33.8 ($C(CH_3)_3$), 31.0, 30.8, 30.2 and 30.0 ($C(CH_3)_3$). ^{51}V NMR (79 MHz, C_6D_6, ppm): δ -321. Elemental analysis: Calcd. for $C_{53}H_{61}N_2O_4V{\cdot}(CH_2Cl_2)$; C, 71.32; H, 6.48; N, 3.32; Found: C, 71.35; H, 6.39; N, 3.05. ESI-MS (CH_3CN): *m/z* = 781.63 $[V^VO(L2)]^+$, 100%; 1656.70 $\{Na[V^VO(L2)(Cl)]_2\}^+$, *ca*. 30%.

General Procedure for the solution sulfoxidation of thioanisole

The catalytic experiments were carried out at atmospheric pressure, at a constant temperature, in a glass vessel, equipped with magnetic stirrer, thermometer and condenser. In a typical run, the solid catalyst (1 mol%) and thioanisole (1 mmol) were dissolved in the appropriate solvent (4 mL). Then the oxidant (1.2 mmol), hydrogen peroxide (20 wt% aqueous solution) was added to the mixture under stirring. Control experiments were carried out in the absence of catalyst. Samples of the reaction mixture were withdrawn periodically and analyzed on a Jasco HPLC system equipped with a Daicel Chiralpak IA column. The eluent used was hexane:ethyl acetate (60:40) with a flow of 1 mL/min. The calibration curves for each reagent and product, namely sulfide, sulfoxide and sulfone, were determined using similar HPLC procedures and these calibrations used for the quantitative analyses. Diphenylsulfone was used as an internal standard [4e].

General Procedure for X-ray Crystallography

Crystals suitable for single-crystal X-ray analysis were obtained for H_2L2, **4** and **5** as described in the experimental procedures. The data were collected using graphite monochromated Mo-K_α radiation (λ = 0.71073 Å) on a Bruker AXS-KAPPA APEX II diffractometer equipped with an Oxford Cryosystem open-flow nitrogen cryostat. Cell parameters were retrieved using Bruker SMART software and refined using Bruker SAINT on all observed reflections. Absorption corrections were applied using SADABS [23]. The structures were solved using direct methods with programs SHELX-XS [24] and SIR2004 [25] and refined with program SHELXL [24], included in the WINGX-Version 1.80.01 [25] system of programs. All non-hydrogen atoms were refined anisotropically and the hydrogen atoms were inserted in idealized positions and allowed to refine riding on the parent carbon atom. The crystals of **4** and **5** had poor diffracting power leading to poor quality data; even so, the structures have been unequivocally determined. The molecular diagrams were drawn with ORTEP-3 for Windows [27] included in the software package. For crystallographic experimental data and structure refinement parameters see Table 3.

Table 3. Selected crystallographic experimental data and structure refinement parameters for **H_2L2**, **4** and **5**.

	H_2L2	**4**	**5**
Empirical formula	$C_{44}H_{56}N_2O_2$	$C_{44}H_{54}N_2O_3V$	$C_{106}H_{122}N_4O_{13}V_4{\cdot}$ $4(C_4H_{10}O)$
Formula weight	644.90	709.83	2160.31
Temperature (K)	150(2)	150(2)	150(2)
Crystal system	Monoclinic	Triclinic	Monoclinic

Space group	$P2_1/c$	*P*-1	*C*2/c
a(Å)	17.2649(9)	14.564(3)	24.146(3)
b(Å)	11.1317(6)	15.406(3)	27.289(3)
c(Å)	10.4440(5)	20.454(3)	18.3902(19)
α(°)	90	93.228(11)	90
β(°)	104.493(3)	101.993(10)	92.886(6)
γ(°)	90	98.017(10)	90
V(Å^3)	1943.34(17)	4428.1(13)	12102(2)
Z, ρ_{calc} (gcm^{-3})	2, 1.102	4, 1.065	4, 1.186
μ(mm^{-1})	0.066	0.260	0.361
Crystal size	0.30×0.26×0.20	0.10×0.04×0.02	0.16×0.16×0.16
Crystal colour	colourless	green	blue
Crystal shape	prism	plate	block
Refl. collected	36138	34664	48184
Unique refl. [R(int)]	4309 [0.0793]	15552 [0.2563]	10605 [0.1798]
R1 [I>2σ(I)]	0.0602	0.1068	0.1100
wR2 [I>2σ(I)]	0.1814	0.2230	0.2638
GooF	1.099	0.808	1.009

Supporting Information

Data for the structures of **H_2L2**, **4** and **5** were deposited in CCDC under the deposit numbers CCDC 1833347-1833349 and can be obtained free of charge from The Cambridge Crystallographic Data Centre via www.ccdc.cam.uk/data_request/cif.

Acknowledgements

The authors thank the Fundação para a Ciência e a Tecnologia, Lisbon, Portugal, for funding (SFRH/BPD/73941/2010, SFRH/BPD/79778/2011, SFRH/BPD/86815/2012, UID/QUI/00100/2013 and RECI/QEQ-QIN/0189/2012) and IST-UL Centers of the Portuguese NMR and Mass Spectrometry Networks (REM2013, RNNMR).

References

[1] K. P. Bryliakov, Chem. Rev. 117 (2017) 11406-11459.

[2] a) H. Pellisier, Coord. Chem. Rev. 284 (2015) 93-110; b) S. Dekar, K. Ouari, S. Bendia, D. Hannachi, J. Weiss, J. Organometal. Chem. (doi.org/10.1016/j.jorganchem.2018.04.015); c) W. A. Zoubi, Y. G. Ko, Appl. Organomet. Chem. 31 (2017) e3574.

[3] a) F. v. d. Velde, I. W. C. E. Arends, R. A. Sheldon, J. Inorg. Biochem. 80 (2000) 81-89; b) S. Takizawa, H. Gröger, H. Sasai, Chem. Eur. J. 21 (2015) 8992-8997.

[4] a) K. Nakajima, M. Kojima, J. Fujita, Chem. Lett. (1986) 1483-1486; b) P. Bravo, M. Crucianelli, A. Farina, S. V. Meille, A. Volonterio, M. Zanda, Eur. J. Org. Chem. (1998) 435-440; c) S. Nakamura, Y. Watanabe, T. Toru, J. Chem. Soc., Perkin Trans. 1 (1999) 3403-3404; d) H. Cotton, T. Elebring, M. Larsson, L. Li, H. Sorensen, S. v. Unge, Tetrahedron: Asymm. 11 (2000) 3819-3825; e) M. Mba, M. Pontini, S. Lovat, C. Zonta, G. Bernardinelli, P. E. Kundig, G. Licini, Inorg. Chem. 47 (2008) 8616-8618; f) P. Adão, J. C. Pessoa, R. T. Henriques, M. L. Kuznetsov, F. Avecilla, M. R. Maurya, U. Kumar, I. Correia, Inorg. Chem. 48 (2009) 3542-3561.

[5] a) S. Nakamura, Y. Watanabe, T. Toru, J. Chem. Soc., Perkin Trans. 1 (1999) 3403-3404; b) H. Cotton, T. Elebring, M. Larsson, L. Li, H. Sorensen, S. v. Unge, Tetrahedron: Asymm. 11 (2000) 3819-3825.

[6] F. Madeira, S. Barroso, S. Namorado, P. M. Reis, B. Royo, A. M. Martins, Inorg. Chim. Acta 383 (2012) 152-156; b) S. Barroso, A. M. Coelho, P. Adão, M. J. Calhorda, A. M. Martins, *Dalton Trans.* 2017,46, 9692-9704; c) S. Barroso, F. Madeira, M. J. Calhorda, M. J. Ferreira, M. T. Duarte, A. M. Martins, Inorg. Chem., 2013, 52, 9427-9439.

[7] a) C. Bolm, F. Bienewald, Angew. Chem. Intl. Ed. 34 (1995) 2640-2641; b) J. Skarzewski, E. Ostrycharz, R. Siedlecka, Tetrahedron: Asymm. 10 (1999) 3457-3461; c) A. G. J. Ligtenbarg, R. Hage, B. L. Feringa, Coord. Chem. Rev. 237 (2003) 89-101; d) C. Drago, L. Caggiano, R. F. W. Jackson, Angew. Chem. Intl. Ed. 44 (2005) 7221-7223; e) M. Hinch, O. Jacques, C. Drago, L. Caggiano, R. F. W. Jackson, C. Dexter, M. S. Anson, S. J. F. MacDonald, J. Mol. Catal. A: Chemical 251 (2006) 123-128; f) H. Liu, M. Wang, Y. Wang, R. Yin, W. Tian, L. Sun, Appl. Organometal. Chem. 22 (2008) 253-257; g) Y. Wang, M. Wang, X. Wang, L. Wang, L. Sun, J. Catal. 273 (2010) 177-181; h) S. Barroso, P. Adão, F. Madeira, M. T. Duarte, J.C. Pessoa, A. M. Martins, Inorg. Chem. 49 (2010) 7452-7463.

[8] a) C. J. Schneider, J. E. Penner-Hahn, V. L. Pecoraro, J. Am. Chem. Soc. 130 (2008) 2712-2713; b) V. Conte, A. Coletti, B. Floris, G. Licini, C. Zonta, Coord. Chem. Rev. 255 (2011) 2165-2177; c) D. Balcells, F. Maseras, G. Ujaque, J. Am. Chem. Soc. 127 (2005) 3624-3634.

[9] a) R. Sanzenbacher, A. Bottcher, H. Elias, Inorg. Chem. 35 (1996) 7493-7499; b) C. S. Higham, D. P. Dowling, J. L. Shaw, A. Cetin, C. J. Ziegler, J. R. Farrell, Tetrahedron Lett. 47 (2006) 4419-4423.

[10] a) K. Bernardo, A. Robert, F. Dahan, B. Meunier, New J. Chem. 19 (1995) 129-131; b) K. Bernardo, S. Leppard, A. Robert, G. Commenges, F. Dahan, B. Meunier, Inorg. Chem. 35 (1996) 387-396; c) P. Muthupandi, S. K. Alamsetti, G. Sekar, Chem. Commun. (2009) 3288-3290; d) N. Madoux, T. Roisnel, V. Dorcet, J. F. Carpentier, Y. Sarazin, Chem. Eur. J. 20 (2014) 6131-6147.

[11] F. H. Allen, O. Kennard, D. G. Watson, L. Brammer, A. G. Orpen, R. Taylor, J. Chem. Soc. Perkin Trans. 2 (1987) S1-S19.

[12] P. Adão, R. Maurya, U. Kumar, F. Avecilla, R. T. Henriques, M. L. Kusnetsov, J. C. Pessoa, I. Correia, Pure Appl. Chem. 81 (2009) 1279-1296.

[13] F. Wolff, C. Lorber, R. Choukroun, B. Donnadieu, Inorg. Chem. 42 (2003) 7839-7845.

[14] a) S. K. Hanson, R. T. Baker, J. C. Gordon, B. L. Scott, A. D. Sutton, D. L. Thorn, J. Am. Chem. Soc. 131 (2009) 428-429; b) S. K. Hanson, R. T. Baker, J. C. Hanson, B. L. Scott, L. A. Silks, D. L. Thorn, J. Am. Chem. Soc. 132 (2010) 17804-17816; c) S. K. Hanson, R. Wu. L. A. Silks, Org. Lett. 13 (2011) 1908-1911; d) G. Zhang, B. L. Scott, R. Wu, L. A. Silks, S. K. Hanson, Inorg. Chem. 51 (2012) 7354-7361.

[15] Z. Liu, F. C. Anson, Inorg. Chem. 39 (2000) 274-280.

[16] a) A. Santalo, F. J. Vidal-Iglesias, J. Solla-Gullón, A. Berná, T. Kallio, J. M. Feliu, Electrochim. Acta 54 (2009) 6576-6583; b) A. Santalo-Aarnio, Y. Kwon, E. Ahlberg, K. Kontturi, T. Kalliu, M. T. M. Koper, Electrochem. Commun. 13 (2011) 466-469.

[17] a) K. Wüthrich, Helv. Chim. Acta 48 (1965) 1012-1017; b) N. D. Chasteen, In *Biological Magnetic Resonance*; Berliner, L. J., Reuben, J., Eds.; Plenum Press: New York, 1981; *Vol. 3*, pp 53−119; c) T. S. Smith II, R. LoBrutto, V. L. Pecoraro, Coord. Chem. Rev. 228 (2002) 1-18.

[18] a) M. Kojima, H. Taguchi, M. Tsuchimoto, K. Nakajima, Coord. Chem. Rev. 237 (2003) 183-196; b) O. Taheri, M. Behzad, A. Ghaffari, M. Kubicki, G. Dutkiewicz, A. Bezaatpour, H. Nazari, A. Khaleghian, A. Mohammadi, M. Salehi, Transition Met. Chem. 39 (2014) 253-259.

[19] a) W. Priebsch, D. Rehder, Inorg. Chem. 29 (1990) 3013-3019; b) D. C. Crans, R. A. Felty, H. Chen, H. Eckert, N. Das, Inorg. Chem. 33 (1994) 2427-2438.

[20] a) P. B. Chatterjee, S. Bhattacharya, A. Audhya, K.-Y. Choi, A. Endo, M. Chaudhury, Inorg. Chem. 47 (2008) 4891-4902; b) Y. N. Belokon, W. Clegg, R. W. Harrington, V. I. Maleev, M. North, M. O. Pujol, D. L. Usanov, C. Young, Chem. Eur. J. 15 (2009) 2148-2165.

[21] A search using CCDC ConQuest program version 1.19 returned 38 hits with the following bond distance ranges for oxidovanadium(V) salen complexes: V=O 1.539 – 1.609 Å, V-$O_{phenolate}$ 1.786 – 2.011 Å, V-O_{imine} 2.054 – 2.114 Å.

[22] A. Rockenbauer, L. Korecz, Appl. Magn. Reson. 10 (1996) 29-43.

[23] G. M. Sheldrick, *SADABS, Program for Empirical Absorption Correction*; University of Göttingen: Göttingen, Germany, 1996.

[24] a) G. M. Sheldrick, , *SHELXL-97 – Programs for Crystal Structure Analysis (Release 97-2)*, Göttingen, Germany, 1998; b) G. M. Sheldrick, Acta Crystallogr. A64 (2008) 112-122.

[25] M. C. Burla, R. Caliandro, M. Camalli, B. Carrozzini, G. L. Cascarano, L. De Caro, C. Giacovazzo, G. Polidori, R. Spagna, J. Appl. Crystallogr. 38 (2005) 381-388.

[26] L. J. Farrugia, J. Appl. Crystallogr. 32 (1999) 837-838.

[27] L. J. Farrugia, J. Appl. Crystallogr. 30 (1997) 565-565.

Text for TOC

New salan- and salen-vanadium complexes display high activity and selectivity in sulfoxidation of thioanisole. Salan-type complexes perform better. Well-defined binaphthyl-based salen complexes display better catalytic performance than *in-situ* prepared systems using [$VO(acac)_2$] and the ligand precursor.

Graphical Abstract

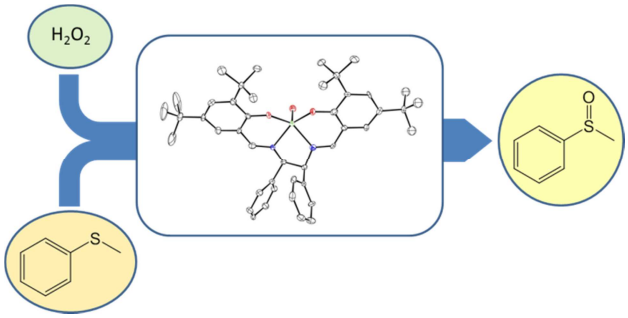

New Salan and Salen Vanadium Complexes: Syntheses and Application in Sulfoxidation Catalysis

Minaxi S. Maru, Sónia Barroso, Pedro Adão, Luis G. Alves and Ana M. Martins*

Centro de Química Estrutural, Instituto Superior Técnico, Universidade de Lisboa, Av. Rovisco Pais 1, 1049-001 Lisboa, Portugal

E-mail: ana.martins@tecnico.ulisboa.pt

Highlights:

- New vanadium complexes of salan- and salen-types are described
- Salen V(V) complexes spontaneously reduce to V(IV) through intramolecular redox processes
- Vanadium salen and salan oxido complexes were assessed as sulfoxidation catalysts
- The inclusion of a binaphthyl moiety in the ancillary ligand frame led to 100% selectivity in sulfoxide